Combustion and Flame 160 (2013) 2800–2809

Contents lists available at SciVerse ScienceDirect

Combustion and Flame

journal homepage: www.elsevier.com/locate/combustflame

The effect of gravity and thermal expansion on the propagation of a triple flame in a horizontal channel

Philip Pearce, Joel Daou *

School of Mathematics, University of Manchester, Manchester M13 9PL, UK

ARTICLE INFO

Article history:
Received 19 February 2013
Received in revised form 17 May 2013
Accepted 9 June 2013
Available online 12 July 2013

Keywords:
Triple-flame
Buoyancy effects
Flame propagation

ABSTRACT

We investigate the effect of thermal expansion and gravity on the propagation of a triple flame in a horizontal channel with porous walls, where the fuel and oxidiser concentrations are prescribed. The triple flame therefore propagates in a direction perpendicular to the direction of gravity, a configuration that does not seem to have received any dedicated investigation in the literature. In particular, we examine the effect of the non-dimensional flame-front thickness ϵ on the propagation speed of the triple flame for different values of the thermal expansion coefficient α and the Rayleigh number Ra. When gravity is not accounted for ($Ra = 0$), and for small values of ϵ, the numerically calculated propagation speed is found to agree with predictions made in previous studies based on scaling laws [1]. We show that the well known monotonic relationship between U and ϵ, which exists in the constant density case when the Lewis numbers are of order unity or larger, persists for triple flames undergoing thermal expansion. Under strong enough gravitational effects ($Ra \gg 1$), however, the relationship is no longer found to be monotonic. For a fixed value of ϵ, the relationship between the Rayleigh number and the propagation speed is shown to vary qualitatively depending on the value of ϵ chosen, exhibiting hysteresis if ϵ is small enough and displaying local maxima, local minima or monotonic behaviour for other values of ϵ. All of the steady solutions presented in the paper have been found to be stable, except for those on the middle branches of the hysteresis curves.

1. Introduction

The study of triple flames, which consist of two premixed branches and a trailing diffusion flame, has been extensive since their first experimental observation by Phillips [2]. Early analytical studies were carried out by Ohki and Tsuge [3], followed by Dold and collaborators [4,5]. These initial studies utilised the constant density approximation, thus decoupling the underlying hydrodynamics of the system from the equations of heat and mass. Most analytical studies since have used this approximation while investigating several practical aspects affecting triple flames. These aspects include preferential diffusion [6,7], heat losses [8–10], reversibility of the chemical reaction [11,12] and the presence of a parallel flow [13]. For further references see the review papers [14,15].

In this paper we dispense with the constant density approximation in order to describe the coupled effect of thermal expansion and gravity on the propagation of the triple flame. To this end, it is imperative to first understand this effect on the "strongly burning" diffusion flame, which forms one of the triple flame's branches. Steadily propagating triple flames are only expected for parameter values for which the diffusion flame exists and is stable.

The diffusive-thermal instability of a planar diffusion flame in the constant density approximation is well studied [16–25], whereby cellular instabilities arise if the fuel and oxidiser Lewis numbers take values smaller than unity and oscillatory instabilities occur if the Lewis numbers take values larger than unity. The effect of thermal expansion on this instability was recently investigated by including the full hydrodynamics in the governing equations [26]. In all cases a planar diffusion flame has been found to be stable if the values of the Lewis numbers are equal and unity, which we take to be the case in the numerical calculations performed in this paper. We have previously undertaken a comprehensive study on the stability of a diffusion flame under the influence of gravity and thermal expansion in the channel configuration adopted in the present paper [27]. There is thus a clear understanding of the values that the parameters can take to ensure the existence and stability of the trailing diffusion flame.

The first attempt to understand the effects of variable density on triple flames was undertaken by Ruetsch et al. [1], who investigated the problem numerically. They have also derived a scaling law describing the increase in the propagation speed of

* Corresponding author.
E-mail addresses: philip.pearce@manchester.ac.uk (P. Pearce), joel.daou@manchester.ac.uk (J. Daou).

0010-2180/$ - see front matter © 2013 The Combustion Institute. Published by Elsevier Inc. All rights reserved.
http://dx.doi.org/10.1016/j.combustflame.2013.06.017

the triple flame above the planar premixed flame speed due to thermal expansion. The increase was attributed to the divergence of the flow field ahead of the flame. The result was confirmed in [28] using numerical simulation; further related numerical studies were carried out in [29–32].

Triple flames propagating in a direction parallel to the direction of gravity have been investigated numerically and experimentally in [33–36]. It has been found that the propagation speed of a triple flame propagating downwards is decreased in comparison to that of a triple flame in the absence of gravity. The change in the propagation speed has been explained in [35] as being due to an increase in the acceleration of the gas ahead of the triple flame leading edge, caused by buoyancy. Conversely, upward propagation leads to an increase in the propagation speed. To our knowledge no dedicated studies have been undertaken on triple flames propagating in a direction perpendicular to gravity.

In the present paper we investigate the combined effect of thermal expansion and gravity on the propagation of a triple flame in a horizontal channel with porous walls, where the fuel and oxidiser concentrations are prescribed. The problem is formulated in the low Mach number approximation. The main aim is to describe the behaviour of the triple flame in terms of three non-dimensional parameters; the flame-front thickness, the thermal expansion coefficient and the Rayleigh number.

The paper is structured as follows. In Section 2 we provide a non-dimensional formulation of the problem. In Section 3 we present some important preliminary results used in later discussions, related to the planar premixed flame and to the existence and stability of the planar diffusion flame. In Section 4, we present the numerical results obtained. In particular, the effect of thermal expansion and gravity on a triple flame is described, with special emphasis on the relationship between the propagation speed U and the flame-front thickness ϵ for various values of the thermal expansion coefficient α and the Rayleigh number Ra. We close the paper with a summary of the main findings and recommendations for future studies.

2. Formulation

We investigate the problem of a triple flame propagating through an infinitely long channel of height L, where fuel is provided at the upper wall and oxidiser at the lower wall, as shown in Fig. 1. The fluid velocity at the walls is assumed to be zero. For simplicity, the walls are taken to be isothermal and of equal temperature. The governing equations consist of the Navier–Stokes equations coupled to equations for temperature and mass fractions of fuel and oxidiser. The combustion is modelled as a single irreversible one-step reaction of the form

$$\mathrm{F} + s\mathrm{O} \rightarrow (1+s)\mathrm{Products} + q,$$

where F denotes the fuel and O the oxidiser. The quantity s denotes the mass of oxidiser consumed and q the heat released, both per unit mass of fuel. The overall reaction rate $\hat{\omega}$ is taken to follow an Arrhenius law of the form

$$\hat{\omega} = \hat{\rho} B \widehat{Y}_F \widehat{Y}_O \exp(-E/R\widehat{T}).$$

Here $\hat{\rho}$, $\widehat{Y}_F$, $\widehat{Y}_O$, R, $\widehat{T}$, B and E are the density, the fuel mass fraction, the oxidiser mass fraction, the universal gas constant, the temperature, the pre-exponential factor and the activation energy of the reaction, respectively.

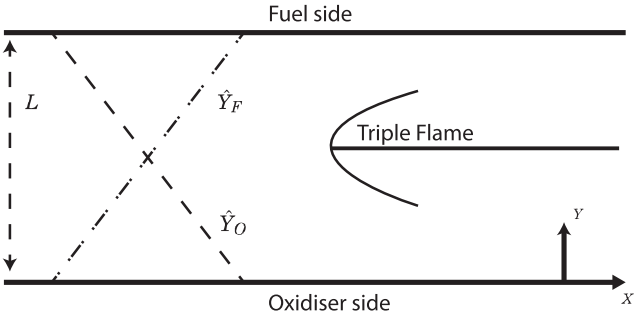

Fig. 1. An illustration of a triple flame in a channel of height L. The walls are assumed to be rigid and to have equal temperatures $\widehat{T} = \widehat{T}_u$. The mass fractions are prescribed by $\widehat{Y}_F = \widehat{Y}_{Fu}, \widehat{Y}_O = 0$ at the upper wall and $\widehat{Y}_F = 0, \widehat{Y}_O = \widehat{Y}_{Ou}$ at the lower wall.

2.1. Governing equations

The governing equations in the low Mach number formulation will be written here using a co-ordinate system attached to the flame front. More precisely, if $\dot{x}_F(\hat{t})$ denotes the propagation speed of the flame front relative to the laboratory (with $\dot{x}_F(\hat{t}) < 0$ indicating a propagation to the left), we shall use the co-ordinates

$$(\hat{t}', X', Y') = (\hat{t}, X - x_F(\hat{t}), Y).$$

This leads to

$$\frac{\partial}{\partial \hat{t}} = \frac{\partial}{\partial \hat{t}'} - \dot{x}_F(\hat{t})\frac{\partial}{\partial X'}.$$

Dropping primes, we write the governing equations as the continuity equation

$$\frac{\partial \hat{\rho}}{\partial \hat{t}} + \frac{\partial}{\partial X}(\hat{\rho}(\hat{u} - \dot{x}_F(\hat{t}))) + \frac{\partial}{\partial Y}(\hat{\rho}\hat{v}) = 0, \tag{1}$$

momentum equations

$$\hat{\rho}\frac{\partial \hat{u}}{\partial \hat{t}} + \hat{\rho}(\hat{u} - \dot{x}_F(\hat{t}))\frac{\partial \hat{u}}{\partial X} + \hat{\rho}\hat{v}\frac{\partial \hat{u}}{\partial Y} + \frac{\partial \hat{p}}{\partial X} = \mu\left(\nabla^2 \hat{u} + \frac{1}{3}\frac{\partial}{\partial X}(\nabla \cdot \hat{\mathbf{u}})\right), \tag{2}$$

$$\hat{\rho}\frac{\partial \hat{v}}{\partial \hat{t}} + \hat{\rho}(\hat{u} - \dot{x}_F(\hat{t}))\frac{\partial \hat{v}}{\partial X} + \hat{\rho}\hat{v}\frac{\partial \hat{v}}{\partial Y} + \frac{\partial \hat{p}}{\partial Y} = \mu\left(\nabla^2 \hat{v} + \frac{1}{3}\frac{\partial}{\partial Y}(\nabla \cdot \hat{\mathbf{u}})\right) + (\hat{\rho} - \hat{\rho}_u)g, \tag{3}$$

temperature equation

$$\hat{\rho}\frac{\partial \widehat{T}}{\partial \hat{t}} + \hat{\rho}(\hat{u} - \dot{x}_F(\hat{t}))\frac{\partial \widehat{T}}{\partial X} + \hat{\rho}\hat{v}\frac{\partial \widehat{T}}{\partial Y} = \hat{\rho} D_T \nabla^2 \widehat{T} + \frac{q}{c_p}\hat{\omega}, \tag{4}$$

fuel and oxidiser mass fraction equations

$$\hat{\rho}\frac{\partial \widehat{Y}_F}{\partial \hat{t}} + \hat{\rho}(\hat{u} - \dot{x}_F(\hat{t}))\frac{\partial \widehat{Y}_F}{\partial X} + \hat{\rho}\hat{v}\frac{\partial \widehat{Y}_F}{\partial Y} = \hat{\rho} D_F \nabla^2 \widehat{Y}_F - \hat{\omega}, \tag{5}$$

$$\hat{\rho}\frac{\partial \widehat{Y}_O}{\partial \hat{t}} + \hat{\rho}(\hat{u} - \dot{x}_F(\hat{t}))\frac{\partial \widehat{Y}_O}{\partial X} + \hat{\rho}\hat{v}\frac{\partial \widehat{Y}_O}{\partial Y} = \hat{\rho} D_O \nabla^2 \widehat{Y}_O - s\hat{\omega}, \tag{6}$$

and the equation of state

$$\hat{\rho}\widehat{T} = \hat{\rho}_u \widehat{T}_u. \tag{7}$$

Here $\hat{p}$ is the hydrodynamic pressure and D_T, D_F, and D_O denote the diffusion coefficients of heat, fuel and oxidiser, respectively. $\widehat{T}_u$ refers to the temperature of the unburnt mixture which is also the temperature of both channel walls, while $\hat{\rho}_u$ is the density of the unburnt mixture. We assume that $\hat{\rho}D_T$, $\hat{\rho}D_F$ and $\hat{\rho}D_O$ are constant, as are the specific heat capacity c_p, thermal conductivity λ and dy-

namic viscosity μ. The flame speed $\dot{x}_F(\hat{t})$ is an eigenvalue of the problem and must be determined as part of the solution.

The conditions as $X \to -\infty$ correspond to the frozen solution with no flow, which is independent of X and is given by

$$\widehat{T} = \widehat{T}_u, \tag{8}$$

$$\widehat{Y}_F = \widehat{Y}_{Fu}\frac{Y}{L}, \tag{9}$$

$$\widehat{Y}_O = \widehat{Y}_{Ou}\left(1 - \frac{Y}{L}\right), \tag{10}$$

$$\hat{u} = \hat{v} = 0, \tag{11}$$

where $\widehat{Y}_{Fu}$ and $\widehat{Y}_{Ou}$ refer to the prescribed mass fractions at the fuel and oxidiser sides respectively. The channel walls are also considered rigid; thus the lateral boundary conditions are

$$\widehat{T} = \widehat{T}_u,\ \widehat{Y}_F = 0,\ \widehat{Y}_O = \widehat{Y}_{Ou},\ \hat{u} = \hat{v} = 0, \quad \text{at } Y = 0, \tag{12}$$

$$\widehat{T} = \widehat{T}_u,\ \widehat{Y}_F = \widehat{Y}_{Fu},\ \widehat{Y}_O = 0,\ \hat{u} = \hat{v} = 0, \quad \text{at } Y = L. \tag{13}$$

Downstream as $X \to \infty$ the solution corresponds to the one-dimensional strongly burning solution of the diffusion flame, which is again independent of X.

For large activation energies, the flame-front region is expected to be centred around the stoichiometric surface $Y = Y_{st}$ where $\widehat{Y}_O = s\widehat{Y}_F$. Upstream, the position of the stoichiometric surface can be determined from Eqs. (8)–(10) as

$$\frac{Y_{st}}{L} = \frac{1}{1+S}, \tag{14}$$

where $S \equiv s\widehat{Y}_{Fu}/\widehat{Y}_{Ou}$ is a normalised stoichiometric coefficient.

We now introduce the non-dimensional variables

$$x = \frac{X}{L}, \quad y = \frac{Y}{L}, \quad u = \frac{\hat{u}}{S_L^0}, \quad v = \frac{\hat{v}}{S_L^0},$$

$$t = \frac{\hat{t}}{L/S_L^0}, \quad \theta = \frac{\widehat{T} - \widehat{T}_u}{\widehat{T}_{ad} - \widehat{T}_u}, \quad y_F = \frac{\widehat{Y}_F}{\widehat{Y}_{F,st}},$$

$$y_O = \frac{\widehat{Y}_O}{\widehat{Y}_{O,st}}, \quad p = \frac{\hat{p}}{\hat{\rho}_u (S_L^0)^2},$$

where the subscript '*st*' denotes values at the upstream stoichiometric surface. Here $\widehat{T}_{ad} \equiv \widehat{T}_u + q\widehat{Y}_{F,st}/c_P$ is the adiabatic flame temperature, $\beta \equiv E(\widehat{T}_{ad} - \widehat{T}_u)/R\widehat{T}_{ad}^2$ is the Zeldovich number or non-dimensional activation energy and $\alpha \equiv (\hat{\rho}_u - \hat{\rho}_{ad})/\hat{\rho}_u$ is the thermal expansion coefficient. In non-dimensionalising we have used as unit speed

$$S_L^0 = \left(4Le_F Le_O \beta^{-3} Y_{O,st}(1-\alpha) D_T B \exp(-E/RT_{ad})\right)^{1/2}, \tag{15}$$

which is the laminar burning speed of the stoichiometric planar flame to leading order for $\beta \gg 1$. Inserting the scalings above into Eqs. (1)–(7) leads to the non-dimensional equations

$$\frac{\partial \rho}{\partial t} + \frac{\partial}{\partial x}(\rho(u + U(t))) + \frac{\partial}{\partial y}(\rho v) = 0, \tag{16}$$

$$\rho\frac{\partial u}{\partial t} + \rho(u + U(t))\frac{\partial u}{\partial x} + \rho v\frac{\partial u}{\partial y} + \frac{\partial P}{\partial x} = \epsilon Pr\nabla^2 u, \tag{17}$$

$$\rho\frac{\partial v}{\partial t} + \rho(u + U(t))\frac{\partial v}{\partial x} + \rho v\frac{\partial v}{\partial y} + \frac{\partial P}{\partial y} = \epsilon Pr\nabla^2 v + \frac{\epsilon^2 PrRa}{\alpha}(1-\rho), \tag{18}$$

$$\rho\frac{\partial \theta}{\partial t} + \rho(u + U(t))\frac{\partial \theta}{\partial x} + \rho v\frac{\partial \theta}{\partial y} = \epsilon\nabla^2\theta + \frac{\epsilon^{-1}\omega}{1-\alpha}, \tag{19}$$

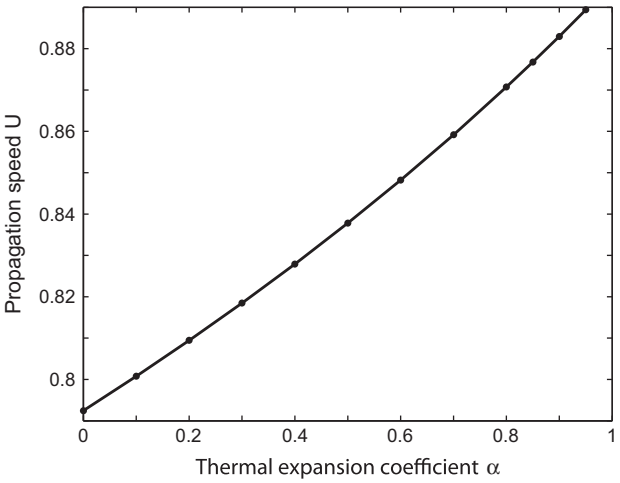

Fig. 3. The effect of the thermal expansion coefficient α on the numerically calculated value of the propagation speed, U_{planar}, for fixed values of the other parameters given by $\beta = 10$, $\epsilon = 1$, $Le_F = Le_O = 1$, $S = 1$, $Pr = 1$ and $Ra = 0$.

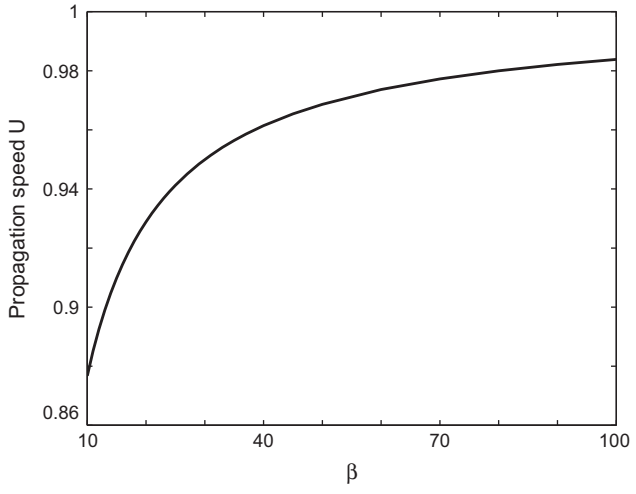

Fig. 2. The effect of β on the numerically calculated value of the propagation speed, U_{planar}, for fixed values of the other parameters given by $\alpha = 0.85$, $\epsilon = 1$, $Le_F = Le_O = 1$, $S = 1$, $Pr = 1$ and $Ra = 0$.

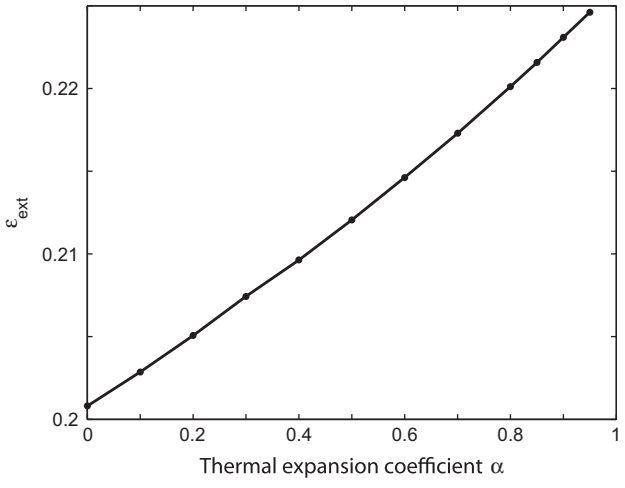

Fig. 4. The effect of the thermal expansion coefficient α on the value of ϵ corresponding to the extinction value of the planar diffusion flame, ϵ_{ext}, for fixed values of the other parameters given by $\beta = 10$, $Le_F = Le_O = 1$, $S = 1$, $Pr = 1$ and $Ra = 0$.

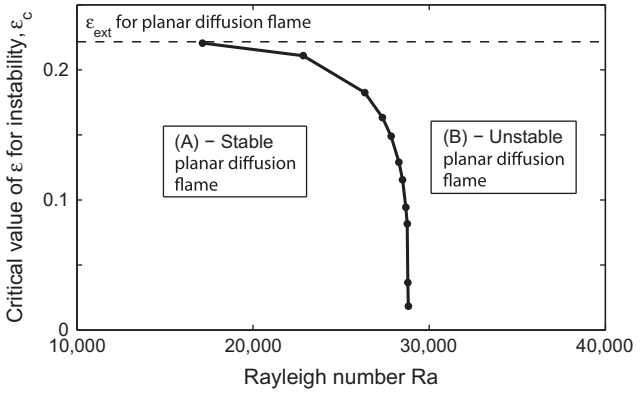

Fig. 5. The effect of the Rayleigh number Ra on the value of ϵ for which the underlying planar diffusion flame becomes unstable, ϵ_c, for fixed values of the other parameters given by $\beta = 10$, $Le_F = Le_O = 1$, $S = 1$, $Pr = 1$ and $\alpha = 0.85$. The two regions in the diagram, labelled A and B, are the regions of stability and instability of the planar diffusion flame, respectively.

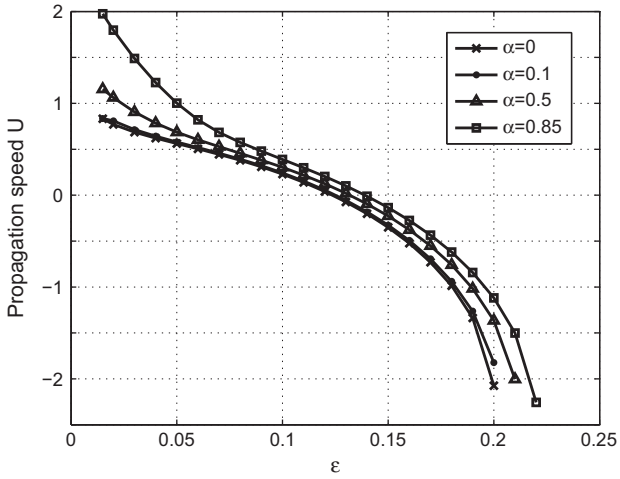

Fig. 6. The effect of ϵ on the propagation speed U for several values of the thermal expansion coefficient α with fixed values of the other parameters given by $\beta = 10$, $Le_F = Le_O = 1$, $S = 1$, $Pr = 1$ and $Ra = 0$. For each α, U is scaled by the numerical value calculated for the propagation speed of the planar premixed flame.

$$\rho\frac{\partial y_F}{\partial t} + \rho(u+U(t))\frac{\partial y_F}{\partial x} + \rho v\frac{\partial y_F}{\partial y} = \frac{\epsilon}{Le_F}\nabla^2 y_F - \frac{\epsilon^{-1}\omega}{1-\alpha}, \tag{20}$$

$$\rho\frac{\partial y_O}{\partial t} + \rho(u+U(t))\frac{\partial y_O}{\partial x} + \rho v\frac{\partial y_O}{\partial y} = \frac{\epsilon}{Le_O}\nabla^2 y_O - \frac{\epsilon^{-1}\omega}{1-\alpha}, \tag{21}$$

$$\rho = \left(1 + \frac{\alpha}{1-\alpha}\theta\right)^{-1}, \tag{22}$$

where P is a modified pressure given by $P = p - \frac{\epsilon Pr}{3}(\nabla\cdot\mathbf{u})$ and $U \equiv -\dot{x}_F/S_L^0$ is the non-dimensional propagation speed relative to the laboratory. The non-dimensional parameters are defined as

$$Ra = \frac{g(\hat{\rho}_u - \hat{\rho}_{ad})L^3}{\nu\hat{\rho}_u D_T}, \quad \epsilon = \frac{l_{Fl}}{L} = \frac{D_T/S_L^0}{L},$$
$$Le_F = \frac{D_T}{D_F}, \quad Le_O = \frac{D_T}{D_O}, \quad \text{and} \quad Pr = \frac{\nu}{D_T},$$

which are the Rayleigh number, the flame-front thickness l_{Fl} measured against the unit length L, the fuel and oxidiser Lewis numbers and the Prandtl number, respectively.

It is worth pointing out that, since L^{-1} is a measure of the mixture fraction gradient in this configuration, the parameter ϵ can be considered as a non-dimensional representation of the latter. More precisely, it can be checked that ϵ is related to the parameter B used in Dold's original analysis of a triple flame [4] by $\epsilon = B/\beta$. Note that ϵ can also be interpreted as defining a Damköhler number by

$$Da = \frac{1}{\epsilon^2(1-\alpha)}.$$

The non-dimensional reaction rate is

$$\omega = \frac{\beta^3}{4Le_F Le_O}\rho y_F y_O \exp\left(\frac{\beta(\theta-1)}{1+\alpha_h(\theta-1)}\right), \tag{23}$$

where α_h is a heat release parameter given by $\alpha_h = (\widehat{T}_{ad} - \widehat{T}_u)/\widehat{T}_{ad}$. Note that in the low Mach number approximation the two parameters $\alpha \equiv (\hat{\rho}_u - \hat{\rho}_{ad})/\hat{\rho}_u$ and α_h are in fact equal, which follows from Eq. (7). In this paper, however, we leave the two distinct to aid comparison of our results with those previously obtained in the constant density approximation [7], where α_h appears in the reaction term ω and only there. To assess the effect of thermal expansion we shall vary the coefficient α, while maintaining $\alpha_h = 0.85$ constant, as in [7,8]. Thus as $\alpha \to 0$ the equations in our study reduce to those of the constant density approximation.[1]

Finally, Eqs. (12) and (13) imply that the boundary conditions are

$$\theta = 0, \tag{24}$$
$$y_F = (1+S)y, \tag{25}$$
$$y_O = \frac{S+1}{S}(1-y), \tag{26}$$
$$u = v = 0 \quad \text{as } x \to -\infty,\ y = 0 \ \text{ or } \ y = 1. \tag{27}$$
$$\frac{\partial u}{\partial x} = \frac{\partial v}{\partial x} = \frac{\partial\theta}{\partial x} = \frac{\partial y_F}{\partial x} = \frac{\partial y_O}{\partial x} = 0 \quad \text{as } x \to +\infty. \tag{28}$$

The non-dimensional problem is now fully formulated and is given by Eqs. (16)–(22) subject to the boundary conditions Eqs. (24)–(28). The non-dimensional parameters in this problem are α, α_h, β, Pr, Ra, ϵ, S, Le_F and Le_O.

3. Preliminary study: the planar premixed flame and the planar diffusion flame

As a preliminary study whose results will be useful for subsequent discussions, in this section we investigate the planar premixed flame and the planar diffusion flame. We will begin with a discussion of how the propagation speed of the planar premixed flame is affected by the parameters α and β. We will then study the planar diffusion flame to determine the values of ϵ, α and Ra for which it is expected to exist in a stable state.

3.1. Planar premixed flame

The equations governing the planar premixed flame are the stationary, y-independent form of Eqs. (16)–(22) subject to the boundary conditions

$$\theta = 0,\ y_F = 1,\ y_O = 0,\ u = v = 0 \quad \text{as} \quad x \to -\infty, \tag{29}$$
$$\frac{\partial u}{\partial x} = \frac{\partial v}{\partial x} = \frac{\partial\theta}{\partial x} = \frac{\partial y_F}{\partial x} = \frac{\partial y_O}{\partial x} = 0 \quad \text{as} \quad x \to +\infty. \tag{30}$$

[1] In asymptotic studies with $\beta \to \infty$, of course α_h is unimportant and can be set to zero. However, for finite values of β, say $\beta = 10$ (which is commonly used in numerical studies), α_h has a noticeable effect.

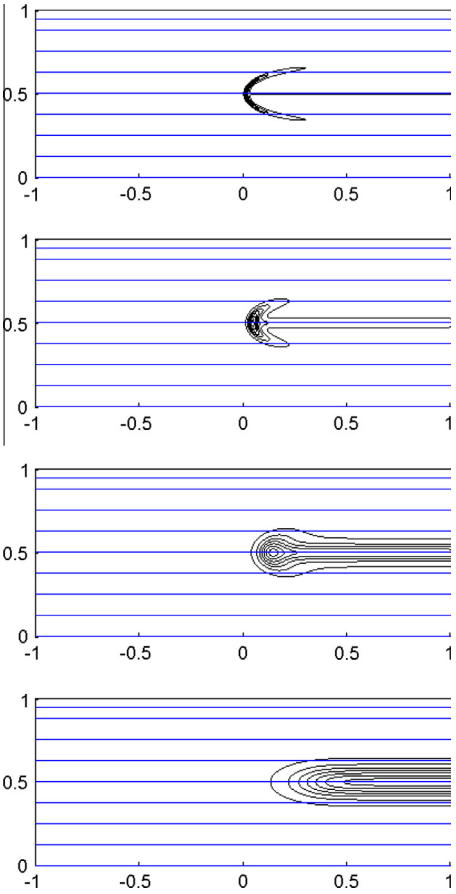

Fig. 7. Streamlines and reaction rate contours in a frame of reference attached to the flame-front for $\alpha = 0$ and $\epsilon = 0.015$, $\epsilon = 0.05$, $\epsilon = 0.12$ and $\epsilon = 0.2$, respectively from top to bottom. The propagation speeds, when scaled by the numerically calculated propagation speed of a planar premixed flame, are given by $U = 0.83$, $U = 0.56$, $U = 0.04$ and $U = -2.07$, respectively.

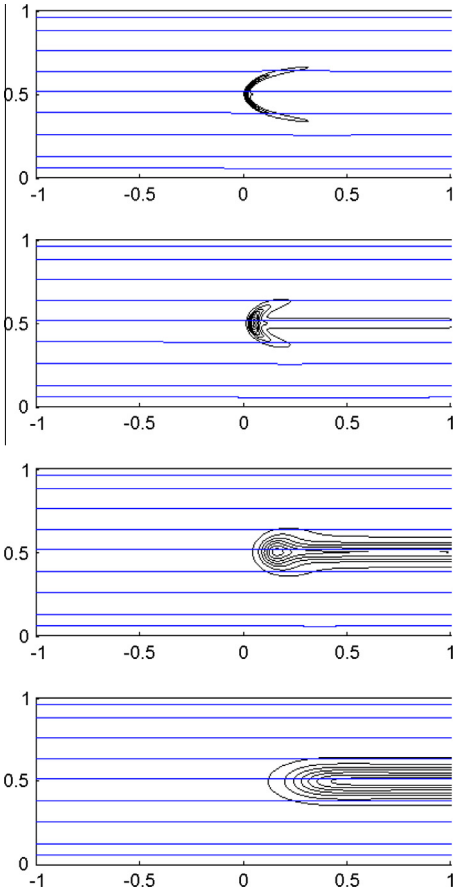

Fig. 8. Streamlines and reaction rate contours in a frame of reference attached to the flame-front for $\alpha = 0.1$ and $\epsilon = 0.015$, $\epsilon = 0.05$, $\epsilon = 0.13$ and $\epsilon = 0.2$, respectively from top to bottom. The propagation speeds, when scaled by the numerically calculated propagation speed of a planar premixed flame, are given by $U = 0.84$, $U = 0.58$, $U = -0.06$ and $U = -1.82$, respectively.

The stationary, one-dimensional problem is solved using the finite-element package Comsol Multiphysics. The aim is to investigate the effect of the parameters α and β on the numerically calculated planar premixed flame propagation speed U_{planar}, which can be compared to its asymptotic value as $\beta \to \infty$. We give the other parameters fixed values of $\epsilon = 1$, $Le_F = Le_O = 1$, $S = 1$, $Pr = 1$, $\alpha_h = 0.85$ and $Ra = 0$.

In the limit $\beta \to \infty$ the (dimensional) propagation speed of the stoichiometric planar flame undergoing thermal expansion should approach the asymptotically derived value S_L^0, given by Eq. (15). Thus, since we have scaled the velocity by this value, the numerically calculated propagation speed U_{planar} should approach unity for all values of α as $\beta \to \infty$. Figure 2 shows that the numerically calculated value of U_{planar} does indeed approach unity with increasing β for a fixed value of $\alpha = 0.85$, as expected.

For the remainder of this paper we let β take a typical value, namely $\beta = 10$. From Fig. 2 it can be seen that for this value of β, the propagation speed U_{planar} deviates from its expected value of unity by about 12%. However, to achieve a notable increase in accuracy would involve significant extra computational cost.

It will also be useful in later discussions to describe how U_{planar} varies with the thermal expansion coefficient α. Figure 3 presents a plot of U_{planar} versus α for a fixed value of $\beta = 10$.

3.2. Planar diffusion flame

Steadily propagating triple flames are not expected if ϵ exceeds the extinction value ϵ_{ext} of the planar diffusion flame. Here we therefore numerically solve the underlying one-dimensional equations independent of x, to produce a plot of ϵ_{ext} versus α, which is provided in Fig. 4.

A plot of the values of ϵ for which the trailing planar diffusion flame becomes unstable under gravity will also be useful in later discussions. This stability problem was investigated in a recent paper [27], from which important results relevant to our study are summarised in Fig. 5. Shown is a plot of the critical value of ϵ versus the Rayleigh number Ra, for $\alpha = 0.85$. This critical value defines the neutral stability curve which separates the two stability regions in the figure. These regions, labelled A and B, define the regions of stability and instability of the planar diffusion flame, respectively.

4. Results for a triple flame propagating in a channel

In this section we present the results obtained by solving the stationary form of Eqs. (16)–(22) with boundary conditions Eqs. (24)–(28) using the finite-element package Comsol Multiphysics. The main aim of the work is to calculate the propagation speed U in terms of the parameters α, ϵ and Ra, which represent thermal expansion, strain rate and gravity, respectively. The other parameters are assigned the values $\beta = 10$, $\alpha_h = 0.85$, $Le_F = Le_O = 1$, $S = 1$ and $Pr = 1$ throughout this section. We begin with an investigation into the effect of thermal expansion on a triple flame in the absence of gravity. This is followed by a study on the combined effects of gas expansion and gravity.

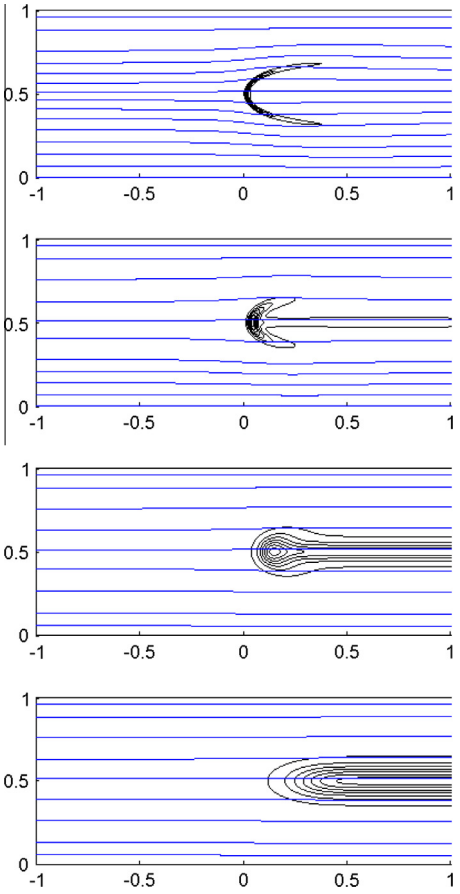

Fig. 9. Streamlines and reaction rate contours in a frame of reference attached to the flame-front for $\alpha = 0.5$ and $\epsilon = 0.015$, $\epsilon = 0.05$, $\epsilon = 0.13$ and $\epsilon = 0.21$, respectively from top to bottom. The propagation speeds, when scaled by the numerically calculated propagation speed of a planar premixed flame, are given by $U = 1.15$, $U = 0.69$, $U = 0.02$ and $U = -2.00$, respectively.

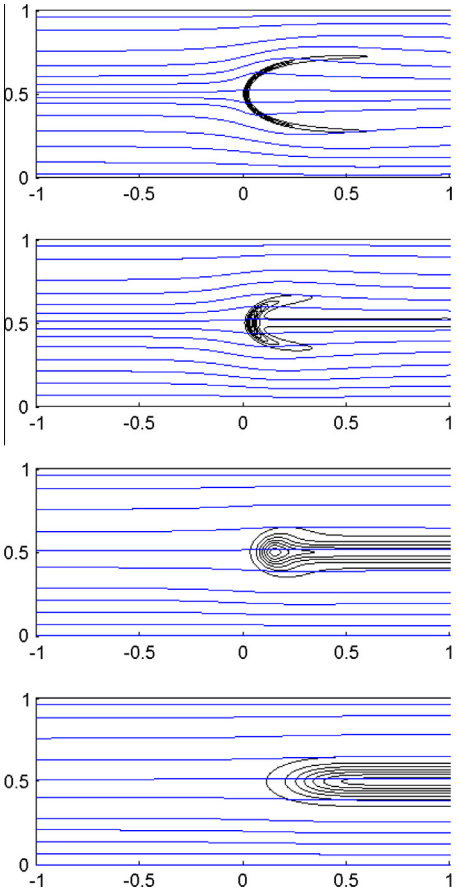

Fig. 10. Streamlines and reaction rate contours in a frame of reference attached to the flame-front for $\alpha = 0.85$ and $\epsilon = 0.015$, $\epsilon = 0.05$, $\epsilon = 0.14$ and $\epsilon = 0.22$, respectively from top to bottom. The propagation speeds, when scaled by the numerically calculated propagation speed of a planar premixed flame, are given by $U = 1.98$, $U = 1.00$, $U = -0.01$ and $U = -2.26$, respectively.

4.1. Effect of thermal expansion on a triple flame in the absence of gravity

In this section we investigate the effect of thermal expansion on a triple flame in the absence of gravity. We therefore let $Ra = 0$ throughout the section. Since the aim of the study is to calculate U, we will begin with a plot of U versus ϵ for several values of the thermal expansion coefficient α. In order to fully understand the effect of the two parameters ϵ and α, we will end with a comparison of how the streamlines and reaction rate contours change with increasing ϵ for several fixed values of α.

4.1.1. Propagation speed of a triple flame

Figure 6 shows a plot of the propagation speed U of the triple flame (scaled by the numerically calculated propagation speed U_{planar} of the planar premixed flame, shown in Fig. 3) versus ϵ for several values of the thermal expansion coefficient α. We begin by noting that the curve labelled $\alpha = 0$ corresponds to the constant density case, which was studied analytically in [13] in the limit $\epsilon \to 0$. We have checked that this curve is consistent with the analytical results of [13] in this limit. The maximum value we let ϵ take for each α is the extinction value ϵ_{ext} of the trailing planar diffusion flame, which can be found in Fig. 4. The monotonic relationship between U and ϵ, with U decreasing to negative values when ϵ is close to ϵ_{ext}, is a well known property of constant density triple flames with Lewis numbers greater than or equal to unity [7]. It is found that this property remains valid for triple flames undergoing thermal expansion, for all values of α, as shown in Fig. 6.

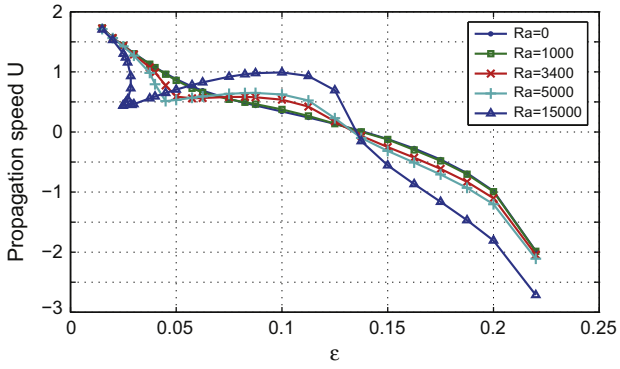

Fig. 11. The effect of ϵ on the propagation speed U for selected values of the Rayleigh number with the values of the other parameters given by $\beta = 10$, $Le_F = Le_O = 1$, $S = 1$, $Pr = 1$ and $\alpha = 0.85$.

It can also be seen in Fig. 6 that, if $\alpha > 0$, U approaches a value larger than that of the planar premixed flame as ϵ approaches zero (i.e. $U/U_{\text{planar}} > 1$ as $\epsilon \to 0$). This result agrees with previous studies, which have found that thermal expansion causes an increase in the propagation speed of a triple flame above the speed of the planar premixed flame [1,28].

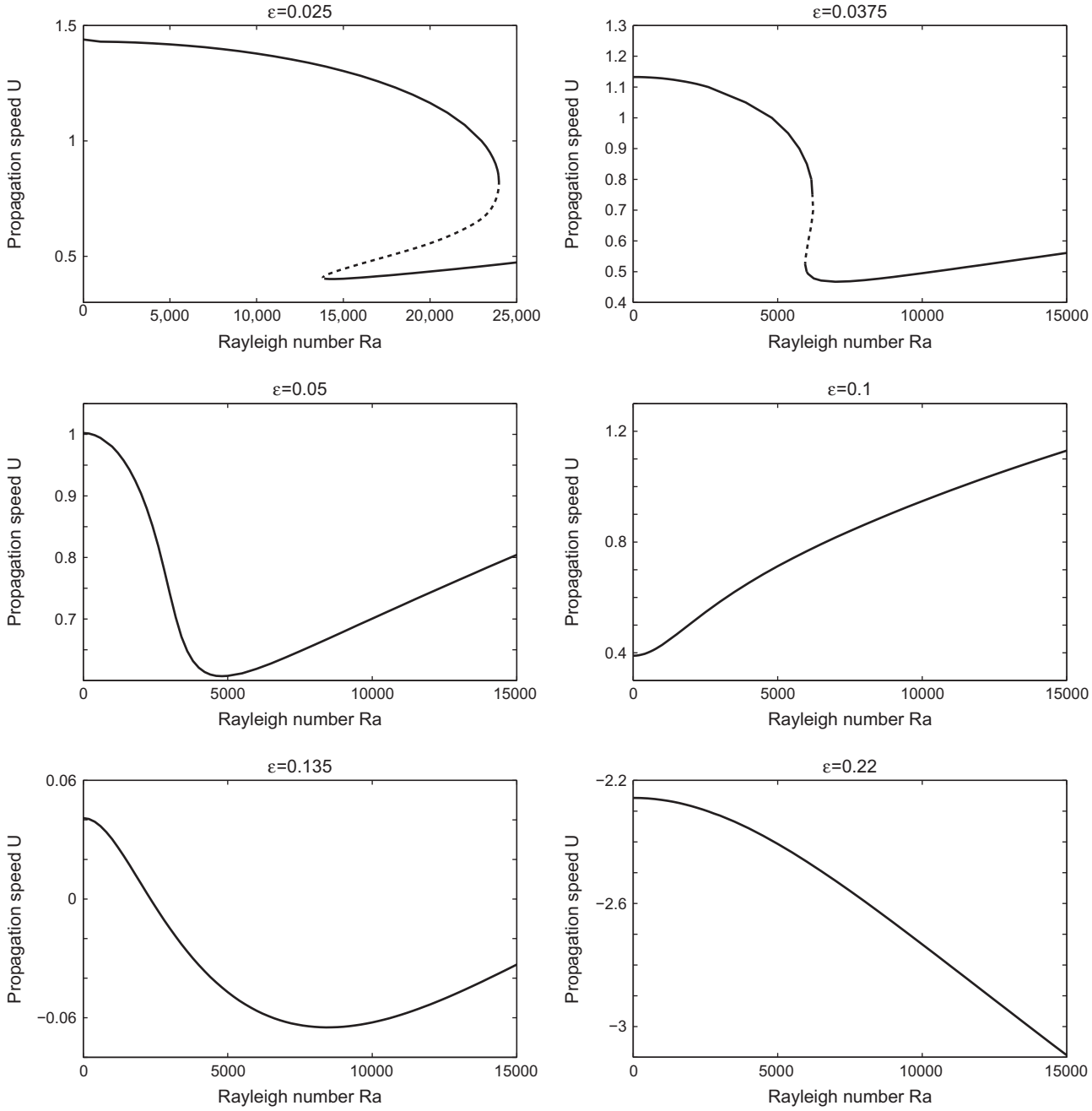

Fig. 12. Comparison of the relationship between propagation speed U and the Rayleigh number Ra for several fixed values of ϵ. The other parameters take fixed values given by $\beta = 10$, $Le_F = Le_O = 1$, $S = 1$, $Pr = 1$ and $\alpha = 0.85$. A dashed line indicates that the steady solutions have been found to be unstable in time-dependent simulations; all other solutions have been found to be stable.

In fact, it can be derived (see [1]) that under the influence of thermal expansion, and in the limit $\epsilon \to 0$, the ratio of the propagation speed of the triple flame to that of the planar premixed flame can be approximated by the formula

$$\frac{U}{U_{\text{planar}}} \sim \left(\frac{\rho_u}{\rho_b}\right)^{1/2} = \left(\frac{1}{1-\alpha}\right)^{1/2} \quad \text{as } \epsilon \to 0. \tag{31}$$

Thus in the case $\alpha = 0.85$, say, the propagation speed of the triple flame (when scaled by the propagation speed of the planar premixed flame) can be expected to approach the value 2.58 as $\epsilon \to 0$. Therefore our results are in good agreement with the predictions made in [1], as can be seen in Fig. 6.

4.1.2. Comparative cases for fixed α

Figures 7–10 show the reaction rate contours and streamlines of the system for increasing values of ϵ, with several fixed values of the thermal expansion coefficient α. Examining, for example, Fig. 10 shows the mechanism for the increase in triple flame speed above that of the planar premixed flame with thermal expansion as $\epsilon \to 0$, discussed in the previous section.

The figure shows that, for small ϵ, ahead of the flame front the streamlines diverge. As explained in detail in [1], the divergence of the streamlines occurs because the fluid velocity normal to the flame front increases with thermal expansion, while the fluid velocity tangential to the flame front remains the same. The flow

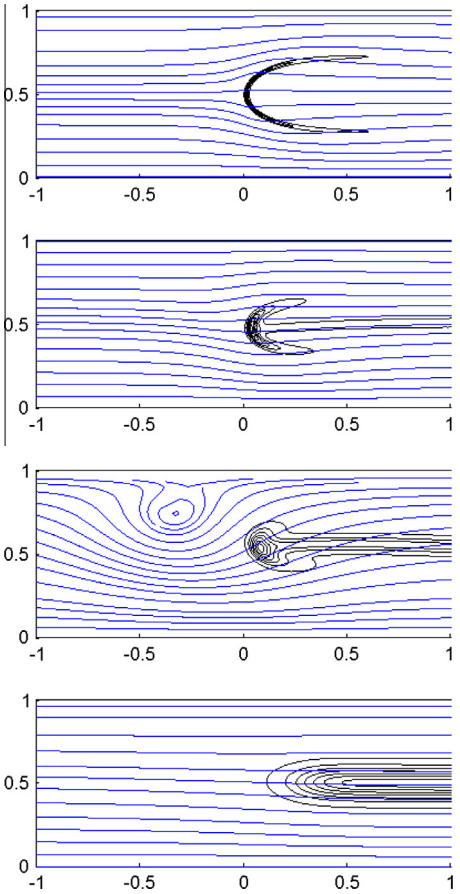

Fig. 13. Streamlines and reaction rate contours in a frame of reference attached to the flame-front for $Ra = 1000$ and $\epsilon = 0.015$, $\epsilon = 0.05$, $\epsilon = 0.1$ and $\epsilon = 0.22$, respectively from top to bottom. The propagation speeds are given by $U = 1.73$, $U = 0.86$, $U = 0.38$ and $U = -1.98$, respectively.

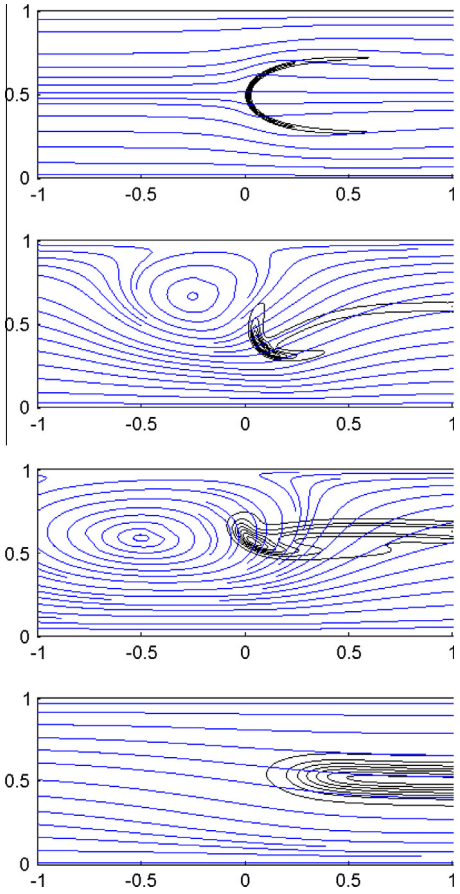

Fig. 14. Streamlines and reaction rate contours in a frame of reference attached to the flame-front for $Ra = 5000$ and $\epsilon = 0.015$, $\epsilon = 0.05$, $\epsilon = 0.1$ and $\epsilon = 0.22$, respectively from top to bottom. The propagation speeds are given by $U = 1.71$, $U = 0.53$, $U = 0.62$ and $U = -2.11$, respectively.

velocity vector is therefore bent towards the centreline (or stoichiometric surface) of the triple flame as it crosses the flame front. This must be accommodated by a divergence of the streamlines, which causes a drop in the horizontal component of the fluid velocity just ahead of the flame front. For small ϵ, since the flame front is quasi-planar, the fluid velocity just ahead of the flame should be approximately equal to the propagation speed of the planar-premixed flame S_L^0. Thus, since the fluid velocity drops ahead of the flame front, the fluid velocity upstream of the flame must be above S_L^0.

4.2. Effect of gravity on a triple flame

In this section we investigate the combined effects of thermal expansion and gravity on a triple flame. Throughout this section we let the thermal expansion coefficient take the typical value $\alpha = 0.85$. Note that we only consider values in parameter space for which the underlying planar diffusion flame is stable, as shown in Fig. 5. Since the aim of the study is to calculate the propagation speed U, we will begin with a plot of U versus ϵ for several values of the Rayleigh number Ra. We will then plot graphs of U versus Ra for selected values of ϵ to further capture the complex relationships that are displayed between the physical parameters and the propagation speed. We will end with a comparison of how the streamlines and reaction rate contours change with increasing ϵ for several fixed values of Ra.

4.2.1. Propagation speed of a triple flame

Figure 11 shows a plot of the propagation speed U of the triple flame versus ϵ, for selected values of the Rayleigh number Ra. The figure shows, firstly, that in the limit $\epsilon \to 0$ the Rayleigh number has very little effect on the propagation speed of a triple flame. This could be easily deduced by considering Eq. (18) and noting that, as $\epsilon \to 0$, the buoyancy term does not enter the problem at $O(1)$ unless $Ra = O(\epsilon^{-2})$. Secondly, the figure shows that there is a critical Rayleigh number, calculated as approximately $Ra = 3400$, above which the graph of U versus ϵ ceases to be monotonic. Finally, it shows the complex behaviour of the system for even higher values of Ra. It is found that there can exist three different steady solutions for some low values of ϵ (i.e. the system exhibits hysteresis). It is also found that at $\epsilon \approx 0.1$, there is a local maximum in the graph of U versus ϵ. As ϵ approaches its extinction value ϵ_{ext}, U is found to fall to negative values as in the case without gravity.

Some of the complex behaviour of the system can be captured by maintaining ϵ fixed and varying Ra. Graphs of U versus Ra for selected values of ϵ are plotted in Fig. 12. In Fig. 12a and b, in which ϵ takes a low value, the hysteresis displayed by the system can be clearly seen, whereby for certain values of Ra there are three solutions for U. The middle branches of these hysteresis curves have been found to consist of unstable solutions. For a slightly higher value of ϵ there is no longer found to be a multiplicity of solutions; the propagation speed has a local minimum at a certain value of Ra before increasing as Ra reaches higher values, as shown in Fig. 12c. In Fig. 12d, in which $\epsilon = 0.1$, U is seen to increase monotonically

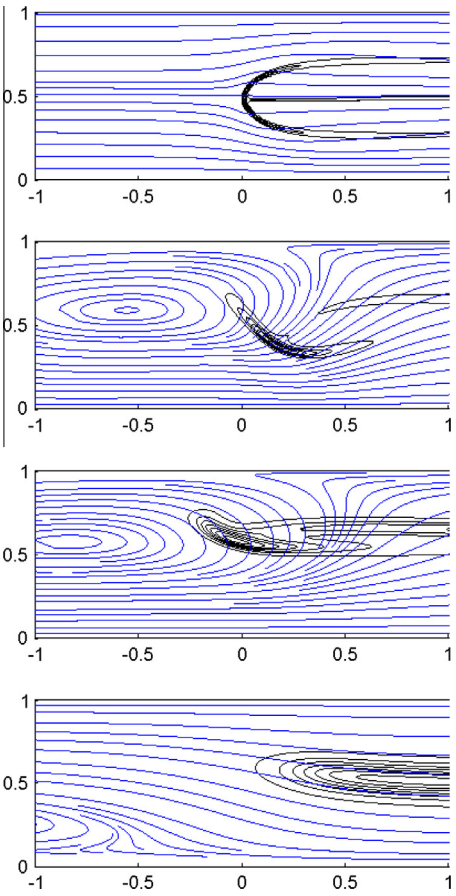

Fig. 15. Streamlines and reaction rate contours in a frame of reference attached to the flame-front for $Ra = 15{,}000$ and $\epsilon = 0.015$, $\epsilon = 0.05$, $\epsilon = 0.1$ and $\epsilon = 0.22$, respectively from top to bottom. The propagation speeds are given by $U = 1.71$, $U = 0.71$, $U = 0.99$ and $U = -2.71$, respectively.

with *Ra*. Figure 12e shows that if $U \approx 0$ for a triple flame without gravity, the propagation speed remains near zero as *Ra* increases. Finally, Fig. 12f shows that when ϵ is near its extinction value (with the propagation speed being negative), *U* decreases monotonically with *Ra*.

For sufficiently small ϵ, as in Fig. 12a–c, it can be seen that *U* decreases with increasing *Ra* for not too large *Ra*. This can be explained by considering the physical behaviour of the system, which we proceed to investigate next.

4.2.2. Comparative cases for fixed Ra

Figures 13–15 show the reaction rate contours and streamlines of the system with increasing values of ϵ, for several fixed values of *Ra*. We begin by noting that the solutions plotted in Figs. 13–15 have all been found to be stable as they do not lie on the middle branch of the hysteresis curves in Fig. 12 discussed in the previous section. From these diagrams it can be seen that buoyancy forces cause the formation of vortices upstream of the flame (or downstream of a negatively propagating triple flame). For higher values of *Ra*, the vortex formed is found to be larger in its size and the strength of its flow.

These vortices can be explained as being caused by the temperature gradient from cold to hot along the positive *x*-direction in the channel. It has been found that in a channel or pipe in the absence of a flame, differentially heated end walls cause the fluid in the channel or pipe to flow from hot to cold along the top of the domain, and from cold to hot along the bottom of the domain [37]. The flow is explained in [37] as being be due to buoyancy forces caused by the change in density with temperature. A similar mechanism can explain the vortices caused by a triple flame in a channel and thus the reduction in the propagation speed of the triple flame for small values of ϵ, when the Rayleigh number is increased above zero. The flow of fluid from hot to cold at the top of the domain and cold to hot at the bottom causes a downward flow in front of a positively propagating triple flame, bending the stoichiometric isosurface ahead of the flame downwards. Effectively this reduces the component of the propagation velocity in the horizontal direction.

More precisely, for small values of ϵ (for which the flame front is quasi-planar), the fluid velocity perpendicular to the flame front across the flame is approximately given by the planar premixed flame speed S_L^0. Thus, when the stoichiometric isosurface ahead of the flame is bent to an angle θ to the horizontal by the downward flow ahead of the flame, the propagation speed can be expected to be approximately $U = S_L^0 \cos\theta$, as shown in Fig. 16. Therefore for small ϵ, an increase in the Rayleigh number (which causes the vortices ahead of the flame to be stronger, and hence bends the stoichiometric isosurface further downwards and increases θ) leads to a decrease in the propagation speed *U*, in the absence of other effects.

This physical behaviour is best illustrated by considering the triple flame under the influence of gravity but in the absence of thermal expansion, so that the acceleration of the flow field as it crosses the triple flame does not mask the effects of buoyancy. To do this, we must make use of the Boussinesq approximation, and expand the ideal gas equation of density, given by Eq. (22), as

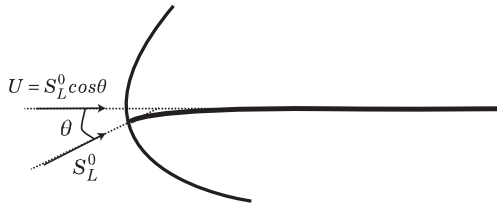

Fig. 16. An illustration of a triple flame for $\epsilon \to 0$ under small gravitational effects. In a frame of reference attached to the triple flame, the fluid flows across the (quasi-planar) flame front at an angle θ to the horizontal at the planar premixed flame speed S_L^0; the fluid velocity along the centreline is therefore smaller than the planar premixed flame speed.

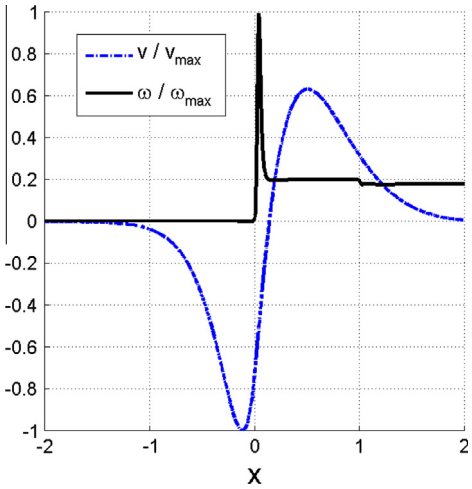

Fig. 17. The vertical component of the velocity vector and the reaction rate along the centreline of the triple flame located at $y = \frac{1}{2}$, both scaled by their maximum values, in the Boussinesq approximation ($\alpha \to 0$) for $\epsilon = 0.05$ and $Ra = 50$. The vertical velocity component is clearly negative just ahead of the flame-front as expected.

$$\rho = 1 - \alpha\theta + O(\alpha^2). \quad (32)$$

This gives $\rho = 1$ to leading order in every term in Eqs. (16)–(21) except the buoyancy term in Eq. (18), which becomes $\epsilon^2 PrRa\theta$.

Now we numerically solve Eqs. (16)–(21) with boundary conditions Eqs. (24)–(28) in the Boussinesq approximation, for a small value of the Rayleigh number, as $\epsilon \to 0$. Plotted in Fig. 17 is the vertical component of the velocity along the centreline of the triple flame located at $y = \frac{1}{2}$. It can be seen that there is a downwards flow upstream of the point where the reaction rate reaches a maximum, and an upwards flow downstream of it. This clearly illustrates the vortex formed by the triple flame and the downwards flow ahead of the flame front.

5. Conclusion

In this study, the effect of thermal expansion and gravity on a triple flame propagating in a horizontal channel where the fuel and oxidiser concentrations are prescribed at the walls has been investigated. This seems to be the first paper dedicated to triple flame propagation in a direction perpendicular to gravity. The problem has been formulated in the low Mach number approximation and solved numerically. The effect of the flame-front thickness ϵ on the propagation speed U has been described for several values of the thermal expansion coefficient α and the Rayleigh number Ra.

It has been found that the well-known monotonic relationship between U and ϵ that is present in the constant density case (which arises in the limit $\alpha \to 0$) remains valid for $\alpha \neq 0$, when $Ra = 0$ (i.e. in the absence of gravity). In fact, the influence of α on the triple flame for $Ra = 0$ is found to agree with the conclusions of the pioneering study [1], where the physical mechanism for the increase in propagation speed has been explained.

Under the influence of gravity we have shown that the monotonic relationship between U and ϵ is only present for values of Ra below a critical value which has been determined. Further, it has been shown that, if Ra takes a value higher than this critical value, there is a local maximum in the graph of U versus ϵ, as can be seen in Fig. 11. The system has been shown to exhibit hysteresis for even higher values of the Rayleigh number.

The complex relationship between U and Ra has been further investigated by fixing ϵ and varying Ra. It has been found that the graph of U versus Ra (see Fig. 12) depends strongly on the value of ϵ chosen. Time-dependent simulations have shown that all of the steady solutions presented are stable, except for solutions on the middle branch of the hysteresis curves presented in Fig. 12. Finally, a physical argument has been provided, which explains the decrease of U with increasing gravity for small values of ϵ.

We believe that the results of this paper provide valuable insight into the behaviour of a triple flame under gravitational effects and illustrate the complexity and variety of the scenarios that arise. A further aspect of the problem which is worth considering in future studies is the time-dependent behaviour of triple flames in situations where the underlying planar diffusion flame is itself unstable due to gravitational effects.

References

[1] G. Ruetsch, L. Vervisch, A. Li ñán, Phys. Fluids 7 (1995) 1447–1454.
[2] H. Phillips, Symposium (International) on Combustion, vol. 10, Elsevier, 1965, pp. 1277–1283.
[3] Y. Ohki, S. Tsuge, in: J.R. Bowen, J.C. Leyer, R.I. Soloukhin (Eds.), Progress in Astronautics and Aeronautics 105 (1986) 233–245.
[4] J. Dold, Combust. Flame 76 (1989) 71–88.
[5] L. Hartley, J. Dold, Combust. Sci. Technol. 80 (1991) 23–46.
[6] J. Buckmaster, M. Matalon, Symposium (International) on Combustion, vol. 22, Elsevier, 1989, pp. 1527–1535.
[7] J. Daou, A. Linán, Combust. Theory Modell. 2 (1998) 449–477.
[8] R. Daou, J. Daou, J. Dold, Combust. Theory Modell. 8 (2004) 683–699.
[9] R. Daou, J. Daou, J. Dold, Proc. Combust. Inst. 29 (2002) 1559–1564.
[10] M. Cha, P. Ronney, Combust. Flame 146 (2006) 312–328.
[11] S. Ali, J. Daou, Proc. Combust. Inst. 31 (2007) 919–927.
[12] J. Daou, Combust. Theory Modell. 13 (2009) 189–213.
[13] J. Daou, F. Al-Malki, Combust. Theory Modell. 14 (2010) 177–202.
[14] J. Buckmaster, Prog. Energy Combust. Sci. 28 (2002) 435–475.
[15] S. Chung, Proc. Combust. Inst. 31 (2007) 877–892.
[16] L. Kirkbey, R. Schmitz, Combust. Flame 10 (1966) 205–220.
[17] S. Cheatham, M. Matalon, AIAA J. 34 (1996) 1403–1409.
[18] J. Kim, F. Williams, P. Ronney, J. Fluid Mech. 327 (1996) 273–301.
[19] S. Cheatham, M. Matalon, Symposium (International) on Combustion, vol. 26, Elsevier, 1996, pp. 1063–1070.
[20] J. Kim, Combust. Theory Modell. 1 (1997) 13–40.
[21] S. Cheatham, M. Matalon, J. Fluid Mech. 414 (2000) 105–144.
[22] S. Kukuck, M. Matalon, Combust. Theory Modell. 5 (2001) 217–240.
[23] R. Vance, M. Miklavcic, I. Wichman, Combust. Theory Modell. 5 (2001) 147–161.
[24] M. Miklavčič, A. Moore, I. Wichman, Combust. Theory Modell. 9 (2005) 403–416.
[25] P. Metzener, M. Matalon, Combust. Theory Modell. 10 (2006) 701–725.
[26] M. Matalon, P. Metzener, J. Fluid Mech. 647 (2010) 453–472.
[27] P. Pearce, J. Daou, J. Fluid Mech. (2013) (submitted for publication).
[28] H. Im, J. Chen, Combust. Flame 119 (1999) 436–454.
[29] V. Katta, W. Roquemore, Combust. Flame 102 (1995) 21–40.
[30] V. Favier, L. Vervisch, Combust. Flame 125 (2001) 788–803.
[31] X. Qin, I. Puri, S. Aggarwal, Proc. Combust. Inst. 29 (2002) 1565–1572.
[32] J. Bieri, V. Kurdyumov, M. Matalon, Proc. Combust. Inst. 33 (2011) 1227–1234.
[33] R. Azzoni, S. Ratti, I. Puri, S. Aggarwal, Phys. Fluids 11 (1999) 3449.
[34] S. Aggarwal, I. Puri, X. Qin, Phys. Fluids 13 (2001) 265.
[35] J. Chen, T. Echekki, Combust. Theory Modell. 5 (2001) 499–515.
[36] T. Echekki, J. Chen, U. Hegde, Combust. Sci. Technol. 176 (2004) 381–407.
[37] A. Bejan, C. Tien, Int. J. Heat Mass Transfer 21 (1978) 701–708.